ISSN 1392–1320 MATERIALS SCIENCE (MEDŽIAGOTYRA). Vol. 12, No. 3. 2006

Effects of the High Temperature Annealing on Structure of the High Velocity Oxygen Fuel Deposited WC-Co Coatings

Šarūnas MEŠKINIS[1*], Judita. PUIŠO[1], Algis JURAITIS[1], Viktoras GRIGALIŪNAS[1], Sigitas TAMULEVIČIUS[1], Romualdas JAKUTIS[2], Arūnas BABILIUS[2]

[1]*Institute of Physical Electronics of Kaunas University of Technology, Savanorių 271, 50131 Kaunas, Lithuania*
[2]*JSC "Technologija", Breslaujos 3B, 44403 Kaunas, Lithuania*

Received 11 February 2006; accepted 17 March 2006

In this study tungsten carbide/cobalt (WC-Co) coatings sprayed by high velocity oxygen fuel (HVOF) deposition were investigated. For the comparative purposes the bulk WC-Co sample cutted from the WC-Co hot roller was studied as well. It was found, that WC-Co bulk sample cutted from the WC-Co hot roller was coated by WO_2 layer as a result of the 900 °C temperature air annealing. No connection between the WC-Co coating oxidation and its peeling as a result of the air annealing was found. The most stable coating in terms of peeling was the most oxidized one. According to XRD analysis, formation of the surface oxide layer inhibits further oxidation of the deeper layer of the coating. Change of the coating morphology was observed as a result of the air annealing starting at 500 °C temperature.
Keywords: WC-Co; HVOF deposition, protective coatings, high temperature air annealing, XRD, SEM.

1. INTRODUCTION

Tungsten carbide/cobalt (WC-Co) coatings deposited by thermal spray technique are widely used as protective layers due to their hardness and high wear-resistance [1]. However, its use for tribological protection of tools and instruments at temperatures higher than 500 °C is complicated. Substantial decrease of the wear resistance of WC-Co coatings was observed at 500 °C temperature [2]. On the other hand, hardness and rupture strength of the bulk WC-Co alloy of the same composition starts to decrease only when ambient temperature exceeds 600 °C [3, 4]. Rapid oxidation of the bulk WC-Co alloys and formation of the WO_3 and $CoWO_4$ oxides at temperatures higher than 600°C was observed in [5]. Despite that WC-Co rolls are widely used for steel hot rolling applications [6] where work temperature can reach 900 °C and more, there are few data on influence of the high temperature air annealing on structure of the WC-Co and related coatings [7]. It must be mentioned, that resistance of the WC-Co coatings to the prolonged wear at 500 °C temperature is worse than wear resistance of the Cr_2C_3-NiCr and CoMoCrSi coatings [8]. However, the main wear of the WC-Co coating occurres during the first 24 hours, while further mechanical treatment results in substantially decreased wear [8]. On the other hand substantial oxidation of WC-NiCrAlSi coating was observed at 700 °C and higher temperatures [9]. However, its high temperature wear resistance was very close to the wear resistance of the oxidation-resistant Cr_2C_3- NiCrAlSi coating [9]. To contribute to the understanding of process taking place during high temperature rolling process, effects of the high temperature air annealing on the structure of the fragments of the bulk WC-Co rolls and thermally sprayed WC-Co coatings were investigated in the present study.

*Corresponding author. Tel.: +370-37-327605; fax: +370-37-314423.
E-mail address: *sarunas.meskinis@fei.lt* (Š. Meškinis)

2. EXPERIMENTAL

In present study WC-Co coatings were grown by high velocity oxygen fuel (HVOF) spray deposition using WC-Co powder. 250 μm – 450 μm thickness coatings were deposited using HVOF spraying system "MicroJet" on steel 45 and steel P6M5 substrates. In all cases WC-Co coatings were deposited onto one side of the steel substrate. Additionally coatings of the 250 μm thickness have been deposited by JetKote high velocity oxygen fuel spraying system. In this case a special rotation mechanism was used. It enabled deposition of the coating on the all four sidelong sides of the rectangle-shaped steel substrate. WC-Co coating deposition conditions are presented in Table 1.

Table 1. Technological parameters of the WC-Co coating deposition process

Gas flux			Powder spray rate (g/min)	Powder composition (mass percents)		
C_3H_8 (l/min)	O_2 (l/min)	N_2 (l/min)		W	C	Co
33.3	142.6	10	35	83	5	12

Thermal processes taking place during hot rolling process were simulated by high temperature air annealing. The samples placed on a special holder were put into the quartz furnace heated to the desirable temperature to ensure sudden increase of the temperature. It is the main difference with [7] research where WC-Co coating was annealed after the steady increase of the temperature. Annealing temperature in the present study was 500, 550, 650, 900 °C. Annealing time – 2 hours. Surface structure and morphology of the samples were investigated after the every annealing.

Phase composition of the samples has been investigated using X-ray diffractometer DRON-3. X-ray tube 2.0

BSV– 24Cu with Cu anode was used as X-ray source. Anode radiation wavelength was $\lambda = 0.154178$ nm. Phase composition of the samples was revealed using a Fullprof software by comparison experimentally measured interplanar distance d and angle of the crystallographic plane reflection in X-ray diffractrogram with data of the JCPDS database [10].

Relative concentration of different chemical elements and compounds was evaluated by comparison of the intensities ratio of the respective X-ray diffraction peaks.

Surface morphology of the samples was investigated using scanning electron microscope JEOL JSM-IC25S.

3. EXPERIMENTAL RESULTS

3.1. XRD study of WC-Co powder

Before deposition, WC-Co powders used for deposition of the coatings were investigated. Structure of WC and W_2C related XRD peaks corresponded to relative concentration of the WC and W_2C 84 % and 9.4 % respectively. No Co related XRD peaks were detected (Fig. 1). However, some unidentified peaks in the diffractogram were found. Absence of the Co related XRD peaks can be explained by presence of the amorphous cobalt phase. Another possible reason would be hindering of the Co crystallites by WC layer: as a result X-ray reflections from the Co crystallographic planes are suppressed.

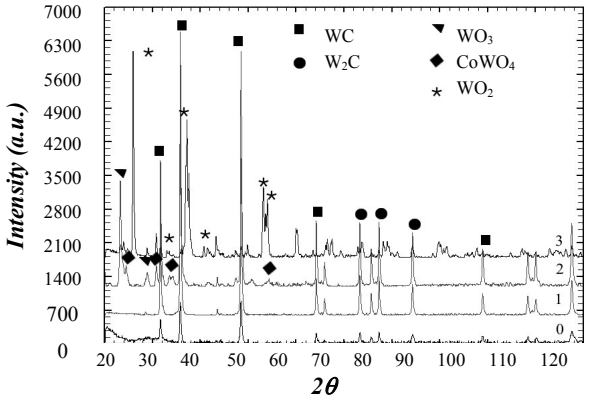

Fig. 1. X-ray diffractogram of the WC-Co powder (0) and fragment of the WC-Co roll (1 – before annealing, 2 – after air annealing at 650 °C temperature, 3 – after air annealing at 900 °C temperature)

3.2. Effects of the air annealing on structure of the bulk WC-Co sample

Diffraction patterns of the bulk WC-Co sample cutted from the WC-Co hot roller are presented in Fig. 1. There are no Co XRD peaks. One can see that composition of the sample according to XRD is 78.8 % WC, 16.4 % W_2C, 5.7 % – unidentified elements and compounds (Table 2). WC concentration decreased from 77.84 % to 65.06 % as a result of 650 °C temperature annealing. Decrease of the amount of W_2C phase was observed as well. It can be explained by processes of the oxidation: WO_3 and $CoWO_4$ appeared in the spectrum. Number of the unidentified peaks increased as well. No X-ray diffraction peaks related to the WC, W_2C, WO_3, $CoWO_4$ can be detected after the 900 °C temperature annealing. On the other hand, peaks of the thermodynamically most stable tungsten oxide – WO_2 appeared.

It must be mentioned, that some tungsten oxide coatings (W_3O type) are harder than thermally sprayed WC-Co coatings (hardness >25 GPa) and it was suggested to use it as a solid lubricant [11]. Therefore, it can be supposed, that formation of the WO_2 takes place only at the surface layer and that newly formed surface layer acts as a high temperature solid lubricant.

Table 2. Effects of the air annealing on phase composition of the fragment of the WC-Co roll

Annealing temperature	Phase structure (%)					
	WC	W_2C	WO_3	$CoWO_4$	WO_2	other
Before annealing	77.84	16.44	0.00	0.00	0.00	5.72
650°C	65.06	10.85	1.09	11.63	0	11.37
900°C	0.00	0.00	0.00	0.00	93.63	6.37

3.3. Effects of the air annealing on the structure of WC-Co coatings

To study air annealing effects, WC-Co coatings of different thickness (250, 350, 400 μm) were deposited onto the steel 45. XRD peaks typical for WC and W_2C can be seen in Fig. 2 – 4. Composition of the coatings was WC 50.5 %– 56 % and W_2C 40 % – 47.5 % (Table 3 – 5). On the other hand in the case of the WC-Co coating deposited onto the high-speed steel P6M5 decrease of the WC concentration as well as formation of the WO_3 (~2 %) and ($CoWO_4$ (~6 %) was observed (Fig. 5, Table 6). It seems, that during the deposition of the coating onto the high speed steel, partial oxidation of the growing layer occurred. After the decomposition of WC, compound of the tungsten with oxygen which is already present in a flame, takes place. Afterwards, as a result of the interaction between the newly formed tungsten oxides with cobalt, $CoWO_4$ is formed. However, it must be taken into the account, that position of the W_2C XRD peak is very close to the position of WO_3 peak. While negligible deviations from stoichiometric composition (formation of W_xC, where x is close to 2) can result in shift of the position of that tungsten carbide peak. Similar behavior was observed for WC-Co coating deposited by JetKote equipment (Fig. 6, Table 7).

Table 3. Effects of air annealing on the phase composition of the 250 μm thickness WC-Co coating deposited onto the steel 45

Annealing temperature	Phase composition (%)				
	WC	W_2C	WO_3	$CoWO_4$	other
Before annealing	50.35	43.72			5.92
500 °C	80.09	19.91	0	0	0
550 °C	47.10	12.79	21.65	18.46	0
650 °C	9.59	5.66	28.15	56.60	0.00

2 hour air annealing at 500 °C temperature resulted in increase of the WC concentration and decrease of the W_2C

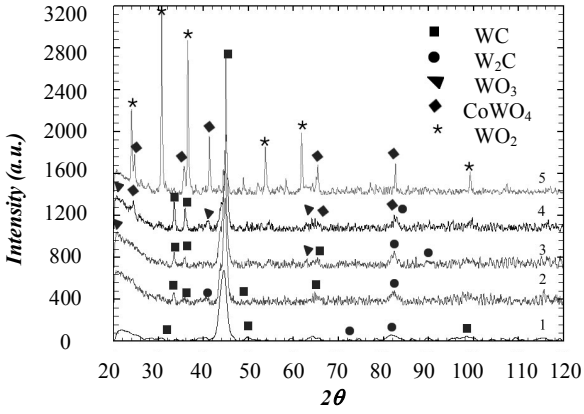

Fig. 2. X-ray diffractogram of the 250 μm thickness WC-Co coating deposited onto the steel 45: 1 – before annealing, 2 – after air annealing at 500 °C temperature, 3 – after air annealing at 550 °C temperature, 4 – after air annealing at 650 °C temperature, 5 – after air annealing at 900 °C temperature

Table 4. Effects of air annealing on the phase composition of the 350 μm thickness WC-Co coating deposited on the steel 45

Annealing temperature	Phase composition (%)				
	WC	W_2C	WO_3	$CoWO_4$	other
Before annealing	56.00	39.48			4.52
500 °C	57.19	36.11	0.00	0.00	6.70
550 °C	66.51	19.48	2.09	4.99	6.93
650 °C	15.08	7.01	26.65	44.22	7.03

Table 5. Effects of air annealing on the phase composition of the 400 μm thickness WC-Co coating grown on the steel 45

Annealing temperature	Phase composition (%)				
	WC	W_2C	WO_3	$CoWO_4$	other
Before annealing	50.51	44.47			5.02
500 °C	11.80	7.65	2.04	76.97	1.54
550 °C	50.03	29.69	0.00	13.44	6.83
650 °C	6.63	1.79	18.33	53.22	20.03

Table 6. Effects of air annealing on the phase composition of the WC-Co coating deposited onto the high speed steel

Annealing temperature	Phase composition (%)				
	WC	W_2C	WO_3	$CoWO_4$	other
Before annealing	55.69	30.7	2.02	6.18	5.41
500 °C	57.18	31.29	0.00	5.62	5.91
550 °C	53.67	27.01	0.00	14.85	4.47
650 °C	18.46	16.28	16.51	38.43	10.32

concentration for 250 μm (Fig. 2, Table 3) and 350 μm thickness (Fig. 3, Table 4) WC-Co coatings deposited onto the steel 45 and WC-Co coating deposited onto the high speed steel. No oxides was observed. In the case of the 250 μm thickness WC-Co coating deposited onto the steel 45 concentration of the WC increased up to 80 %. On the other hand substantial amount of the $CoWO_4$ (60.5 % – 77 %) was observed in the case of 400 μm thickness WC-Co coating deposited on steel 45 (Fig. 4, Table 5) and 250 μm thickness WC-Co coating deposited by JetKote (Fig. 6, Table 7). In the case of the WC-Co coating deposited onto the high speed steel, a wide XRD peak appeared instead of the WO_3 XRD peak (Fig. 5). Such a broadening of the peak indicates formation of some amorphous compound. Therefore, it can not be described by presence of the WO_3. Concentration of $CoWO_4$ slightly decreased (from 6.18 % to 5.62 %) (Table 6). Ratio of the WC and W_2C phases in that coating remained nearly the same after the 500 °C temperature air annealing.

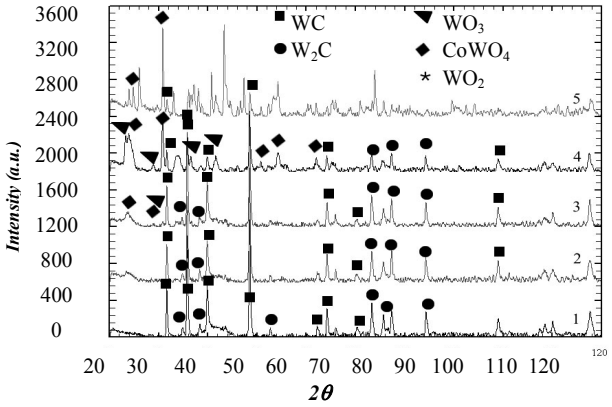

Fig. 3. X-ray diffractogram of the 350 μm thickness WC-Co coating deposited on the steel 45: 1 – before annealing, 2 – after air annealing at 500 °C temperature, 3 – after air annealing at 550 °C temperature, 4 – after air annealing at 650 °C temperature, 5 – after air annealing at 900 °C temperature

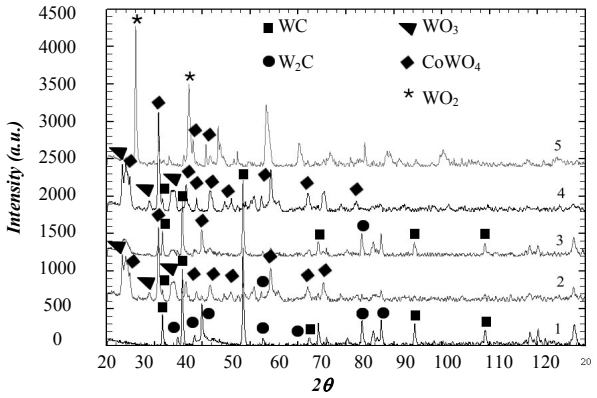

Fig. 4. X-ray diffractogram of the 400 μm thickness WC-Co coating deposited onto the steel 45: 1– before annealing, 2 – after air annealing at 500 °C temperature, 3 – after air annealing at 550 °C temperature, 4 – after air annealing at 650 °C temperature, 5 – after air annealing at 900 °C temperature

According to visual inspection of the samples no spalling only for WC-Co coatings of the 250 μm thickness deposited onto the steel 45 and deposited by JetKote equipment was found. It seems, that spalling of the

coatings can be explained rather by some thermally-induced stress and not by the formation of the oxides.

Table 7. Effects of the air annealing on the phase composition of the WC-Co coating deposited by JetKote equipment.

Annealing temperature	Phase composition (%)				
	WC	W_2C	WO_3	$CoWO_4$	other
Before annealing	40.50	55.19	4.31		
500 °C	5.99	4.92	25.25	60.53	3.31
550 °C	0	0	33.33	66.67	
650 °C	0	0	28.29	54.85	16.86

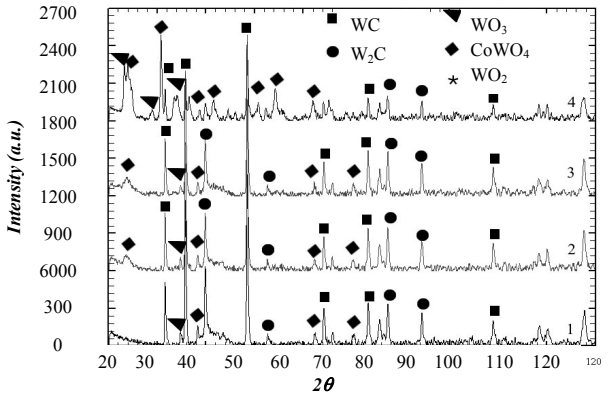

Fig. 5. X-ray diffractogram of the WC-Co coating deposited onto the high speed steel: 1 – before annealing, 2 – after air annealing at 500 °C temperature, 3 – after air annealing at 550 °C temperature, 4 – after air annealing at 650 °C temperature

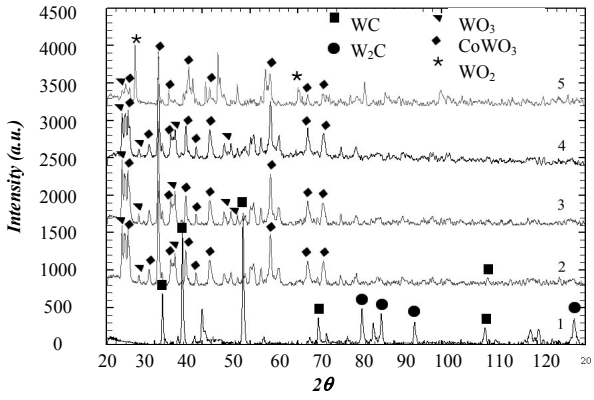

Fig. 6. X-ray diffractogram of the WC-Co coating deposited by JetKote equipment: 1 – before annealing, 2 – after air annealing at 500 °C temperature, 3 – after air annealing at 550 °C temperature, 4 – after air annealing at 650 °C temperature, 5 – after air annealing at 900 °C temperature

Increase of the annealing temperature up to 550 °C resulted in formation of the oxides in the 250 μm thickness WC-Co coating deposited onto the 45 steel (WO_3 – 21.65 %, $CoWO_4$ – 18.46 %) (Fig. 2, Table 3). Less oxides was observed in the case of the 350 μm thickness WC-Co coating (WO_3 – 2.09 %, $CoWO_4$ – 4.99 %) (Fig. 3, Table 4). While concentration of the WC phase even increased. On the other hand, in the case of the 400 μm thickness WC-Co coating, XRD peaks related to WO_3 disappeared (Fig. 4, Table 5). Concentration of $CoWO_4$ substantially decreased as well (from 76.97 % to 13.44 %): some related XRD peaks disappeared, intensity of the others decreased or these peaks were broadened (in that case increase of the noise level related to presence of the amorphous phase was observed). These changes can be partially explained by spalling of the more oxidized parts of the WC-Co coating. No WO_3 related XRD peaks and increase of the $CoWO_4$ concentration from 5.62 % to 14.85 % was observed for WC-Co coating deposited onto the high speed steel substrate (Fig. 5, Table 6). Further oxidation and disappearance of the WC and W_2C related XRD peaks can be seen in the case of the WC-Co coating spray-deposited by JetKote equipment (Fig. 6, Table 7). Visual inspection of the samples revealed spalling for all coatings investigated. It should be mentioned, that the least damaged was coating grown using JetKote spray unit (the most oxidized WC-Co coating).

After the air annealing at 650 °C temperature the most of the crystalline phase consisted of oxides (mostly $WCoO_4$). In the case of the WC-Co coating grown by JetKote equipment large amount of the unidentified compounds was observed (~17 %) (Fig. 6, Table 7). It must be mentioned, that except the coating deposited by JetKote for all the WC-Co coatings substantial peeling or spalling observed.

Number of the unidentified XRD peaks increased as a result of the air annealing at 900 °C temperature. Only part of that peaks can be attributed to the $CoWO_4$ and WO_2. WC-Co coating deposited onto the high speed steel totally spalled despite it was the least oxidized coating after annealing at 650 °C temperature.

It can be mentioned, that steady increase of the annealing temperature resulted in appearance of the WO_3 related XRD peaks at 500 °C temperature and $CoWO_4$ XRD peak at 550 °C temperature [7] while in the case of the fast rise of the annealing temperature it occurred at 500 °C – 550 °C temperature as well. On the other hand steady increase of the annealing temperature resulted in disappearance of the WC and related tungsten carbide peaks already at 650 °C temperature. While in the case of the fast annealing temperature increase only for coatings deposited by JetKote equipment WC and W_2C related XRD peaks disappeared. However it occurred at higher (900 °C) temperature. Despite that, spalling of the steadily annealed WC-Co coating occurred only after annealing at 900 °C temperature.

Such contradictory results can be explained by peculiarities of the XRD measurements. In this method it is possible to receive some information about the coating layer being deeper than 10 μm only in the case if coating is porous or cracked. Therefore, full oxidation of the WC-Co coating deposited by JetKote equipment as a result of air annealing at 550 °C temperature can be understood only as oxidation of the surface layer. In this case it is difficult to predict composition of the coating at 10 μm and higher depth.

3.4. Effects of the air annealing on the surface morphology of the bulk WC-Co sample and WC-Co coatings: SEM study

Illustration of changes of surface morphology of the fragment of WC-Co roll and WC-Co coatings deposited by high velocity oxygen fuel process is presented in Fig. 7 – 9. One can see, that bulk WC-Co sample is less porous as WC-Co coatings. Air annealing at 650 °C and 900 °C temperatures did not change surface morphology of the WC-Co roll fragment. No substantial differences between the all investigated WC-Co coatings were found. Therefore in this article only some SEM images of the 350 μm thickness WC-Co coating deposited onto the 45 steel and WC-Co coating deposited onto the high speed steel are included (Fig. 7, 8). For all investigated WC-Co coatings complex dendrite-like structure was observed. Air annealing at 500 °C temperature resulted in surface morphology changes similar for all WC-Co coatings: coarsening of the surface structure and disappearance of the dendrite-like structure. It must be mentioned, that such a behavior differ from the changes of the coatings phase composition investigated by XRD (Fig. 2 – 6, Table 3 – 7) where for some coatings oxidation was observed while for other there were observed no changes.

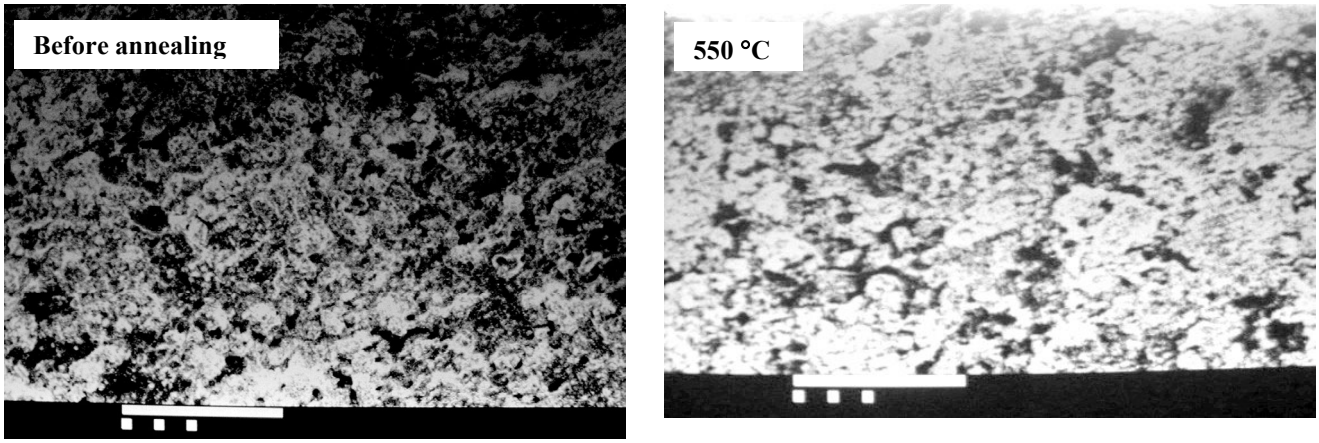

Fig. 7. Air annealing effects on surface morphology of the 350 μm thickness WC-Co coating deposited onto the 45 steel. Size of the mark – 100 μm

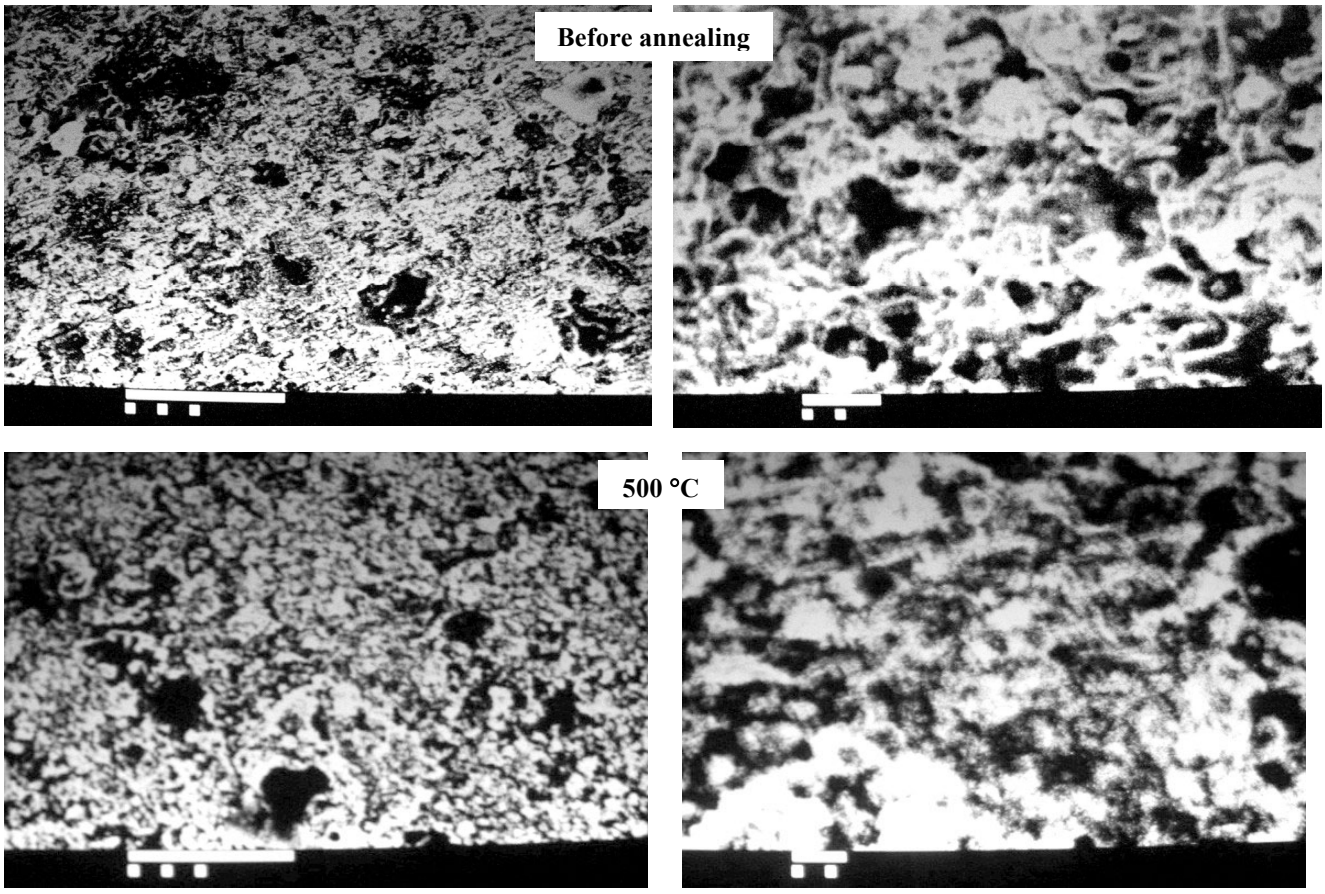

Fig. 8. Air annealing effects on surface morphology of the WC-Co coating deposited onto the high speed steel. Size of the mark with 3 points – 100 μm, size of the mark with 2 points – 10 μm

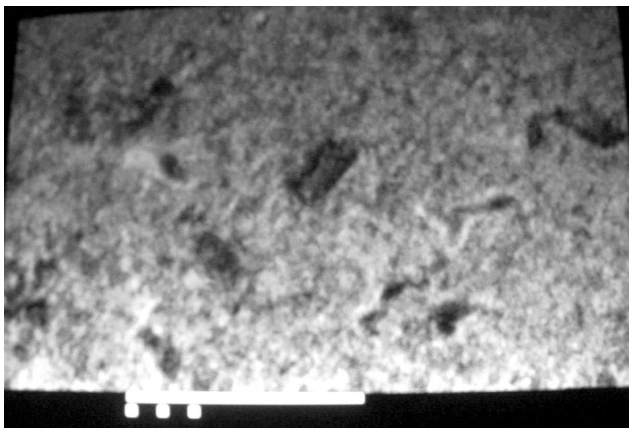

Fig. 9. SEM image of the of the bulk WC-Co sample

CONCLUSIONS

In conclusion effects of the high temperature air annealing on structure and surface morphology of the bulk fragment of the WC-Co roll and WC-Co coatings grown by high velocity oxygen fuel spray deposition were investigated. It was found, that air annealing at 900 °C temperature results in covering of the bulk WC-Co sample by WO_2 layer. No connection between the oxidation of the WC-Co coating and deterioration of the adhesion between the coating and steel substrate as a result of the air annealing was observed. The most resistant to the negative influence of the air annealing coating was the most oxidized as well. It was explained by the formation of the inhibitor oxide layer. No connection between the annealing-induced changes of the surface morphology of the WC-Co coatings and their chemical composition and structure was found. However, changes of the surface morphology similar for all WC-Co coatings as a result of 500^{o}C temperature air annealing were observed.

Acknowledgments

Support of the Lithuanian Sciences and Studies Foundation should be acknowledged.

REFERENCES

1. **He, Jianhong, Schoenung, J. M.** A Review on Nanostructured WC–Co Coatings *Surface and Coatings Technology* 157 2002: pp. 72 – 79.
2. **Babilius, A.** Influence of Temperature on Tungsten Carbide Coating Sprayed by Different Spray Systems *Material Science* (*Medžiagotyra*) 11 2005: pp. 105 – 107.
3. **Acchar, W., Gomes, U. U., Kaysser, W. A., Goring, J.** Strength Degradation of a Tungsten Carbide-Cobalt Composite at Elevated Temperatures *Materials Characterization* 43 1999: pp. 27 – 32.
4. **Milmana, Yu. V., Luyck, S., Northrop, I. T.** Influence of Temperature, Grain Size and Cobalt Content on the Hardness of WC–Co Alloys *International Journal of Refractory Metals and Hard Materials* 17 1999: pp. 39 – 44.
5. **Basu, S. N., Sarin, V. K.** Oxidation Behavior of WC-Co *Materials Science and Engineering A* 209 1996: pp. 206 – 212.
6. http://www.atomat.com/eng/prodotti/hotrolling/tungsten.htm
7. **Babilius, A.** Influence of Temperature on the Phases Changes of HVOF Sprayed Tungsten Carbide Coatings *Materials Science* (*Medžiagotyra*) 9 2003: pp. 183 – 186.
8. **Koiprasert, H., Dumrongrattana, S., Niranatlumpong, P.** Thermally Sprayed Coatings for Protection of Fretting Wear in Land-based Gas-turbine Engine *Wear* 257 2004: pp. 1 – 7.
9. **Berns, H., Koch, S.** High Temperature Sliding Abrasion of a Nickel-Base Alloy and Composite *Wear* 225 – 229 1999: pp. 154 – 162.
10. JSPDS Cards – International Center for Diffraction Data. 12 Campus Boulevard Newtown Square, PA 19073 – 3273 USA.
11. **Lugscheider, E., Knotek, O., Bärwulf, S., Bobzin, K.** Characteristic Curves of Voltage and Current, Phase Generation and Properties of Tungsten- and Vanadium-oxides Deposited by Reactive d.c.-MSIP-PVD-process for Self-lubricating Applications *Surface and Coatings Technology* 142 – 144 2001: pp. 137 – 142.

DOI: 10.5755/j02.ms.26433